Manning River and Clyde River boat wave investigation

WRL TR 2024/13, June 2024

By I R Coghlan, L Montano and J W Chan

UNSW
Water Research
Laboratory

UNSW
SYDNEY

UNSW
Water Research
Laboratory

UNSW
SYDNEY

Manning River and Clyde River boat wave investigation

WRL TR 2024/13, June 2024

By I R Coghlan, L Montano and J W Chan

Project details

Report title	Manning River and Clyde River boat wave investigation
Authors(s)	I R Coghlan, L Montano and J W Chan
Report no.	2024/13
Report status	Final
Date of issue	June 2024
WRL project no.	2021068
Project manager	I R Coghlan
Client	NSW Department of Climate Change, Energy, the Environment and Water
Client address	Building 4, 480 Weeroona Road Lidcombe NSW 2141
Client contact	Adam Wethered adam.wethered@environment.nsw.gov.au
Client reference	#

Document status

Version	Reviewed by	Approved by	Date issued
Draft	FF	BMM	07/05/24
Final	FF	FF	24/06/24

This report should be cited as: Coghlan, IR, Montano, L & Chan, JW 2024, Manning River and Clyde River boat wave investigation, WRL Technical Report 2024/13, UNSW Water Research Laboratory.

UNSW
Water Research
Laboratory

www.wrl.unsw.edu.au
110 King St Manly Vale NSW 2093 Australia
Tel +61 (2) 8071 9800 ABN 57 195 873 179

Executive summary

Data was collected at the Manning River and Clyde River monitoring stations between December 2021 and March 2023. The observed ambient wave climate was very calm at both monitoring stations for almost the entire recording period. Based on the expected range of wave periods for wind waves at these sites and the typical range of boat wave periods, the highest and most energetic waves at both monitoring sites are generated by passing boats.

Although only a very small proportion of waves measured during the deployments at the Manning River and Clyde River sites had wave energy with the potential to cause bank erosion (greater than 50 kg.m/s^2), the largest waves recorded at the Manning River (2,000 kg.m/s^2) and Clyde River (700 kg.m/s^2) sites were an order of magnitude higher than this indicative erosion threshold value.

There were substantially more boats detected on the Manning River compared to the Clyde River during the data collection program. The highest individual waves and maximum individual wave energy were recorded on the Manning River, although maxima values on the Clyde River were not significantly lower.

Contents

List of tables

List of figures

1 Introduction

The Water Research Laboratory (WRL) of the School of Civil and Environmental Engineering at UNSW Sydney was engaged by the NSW Department of Climate Change, Energy, the Environment and Water (DCCEEW; formerly the NSW Department of Planning and Environment) to partner in monitoring boat traffic at one location on the south channel of the Manning River (at Pampoolah) and one location on the upper Clyde River (approximately 7 km downstream of Shallow Crossing) for NSW Local Land Services (LLS). DCCEEW led the project while WRL provided expert assistance by developing and implementing a pilot field program to measure the local wave climate and automatically photograph boat traffic at both sites. DCCEEW staff assisted WRL staff with the initial deployment of a camera and wave probe at each location. Subsequent field trips to maintain and retrieve these instruments (cleaning, data downloads and battery changes) were undertaken by DCCEEW staff with remote support provided by WRL.

2 Site locations and collected data

The monitoring station on the Manning River was located in shallow water adjacent to the right (western) bank (when facing downstream) as shown in Figure 2.1. Instrumentation on the Clyde River was located in similar water depths adjacent to the left (eastern) bank as shown in Figure 2.2.

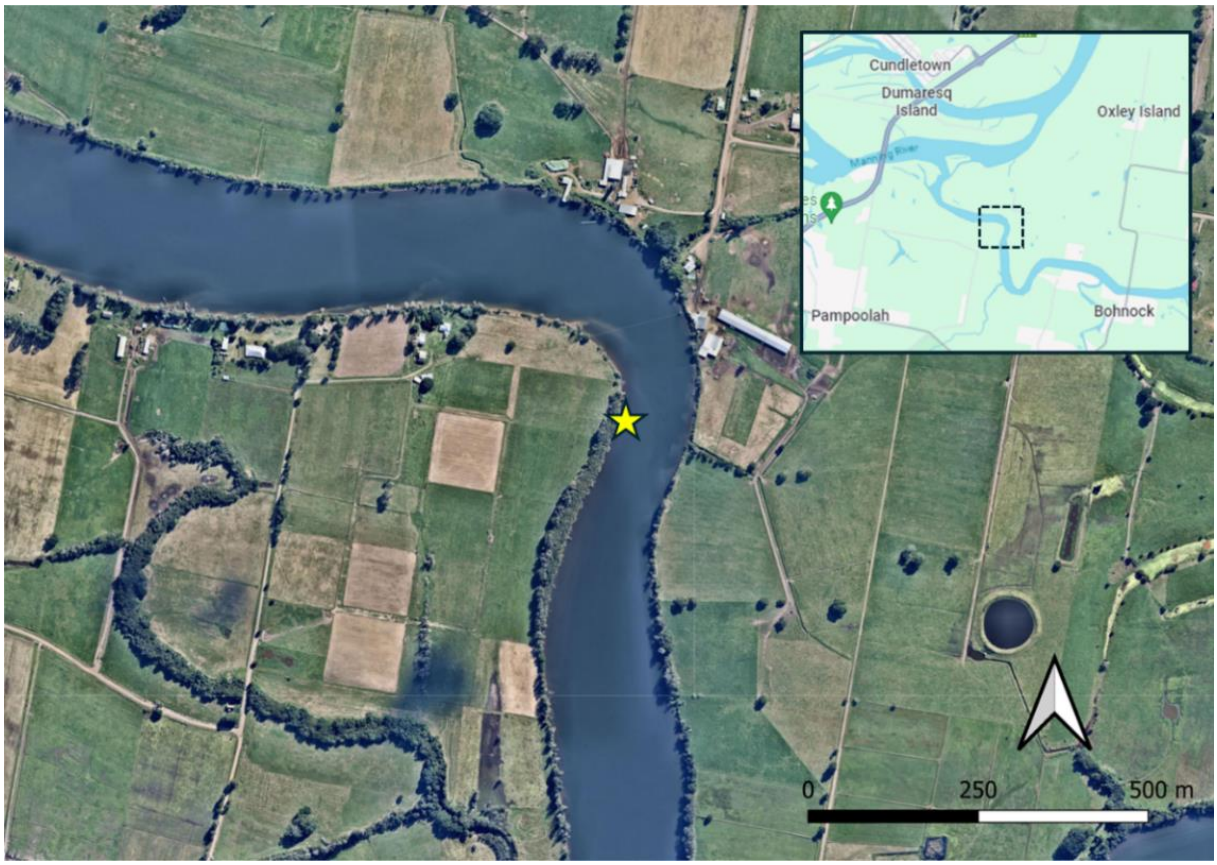

Figure 2.1 Camera and wave probe location on the Manning River

Figure 2.2 Camera and wave probe location on the Clyde River

Table 2.1 summarises the data collection periods between December 2021 and March 2023 for instrumentation on the Manning River and Clyde River. This same information is illustrated in Figure 2.3 and Figure 2.4, respectively. The camera and wave probe generally collected data concurrently at both locations except for 14 December 2022 to 17 February 2023 on the Manning River (wave probe available only) and the early part of the campaign in December 2021 and February and March 2022 on the Clyde River (camera available only).

Table 2.1 Summary of data collection periods on the Manning River and Clyde River

Location	Camera	Wave probe
Manning River	23/03/2022 – 14/12/2022	23/03/2022 – 26/05/2022 (Manning deployment 1) 04/08/2022 – 07/10/2022 (Manning deployment 2) 14/12/2022 – 17/02/2023 (Manning deployment 3)
Clyde River	17/12/2021 – 23/12/2021 10/02/2022 – 30/06/2022 23/12/2022 – 03/03/2023	04/04/2022 – 07/06/2022 (Clyde deployment 1) 19/12/2022 – 22/02/2023 (Clyde deployment 2)

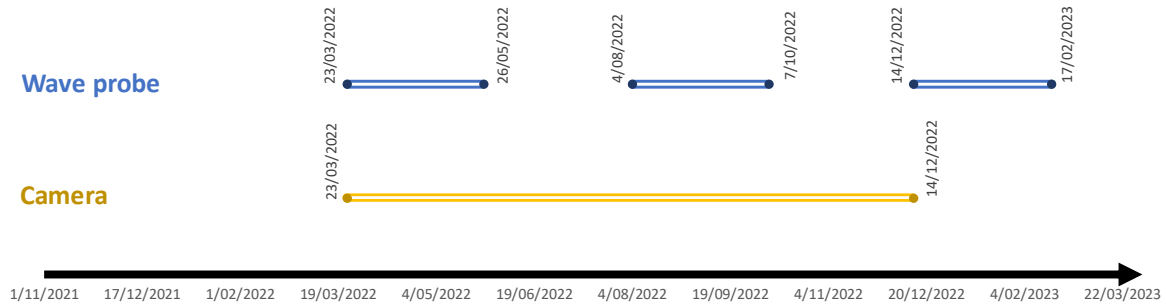

Figure 2.3 Data collection periods on the Manning River

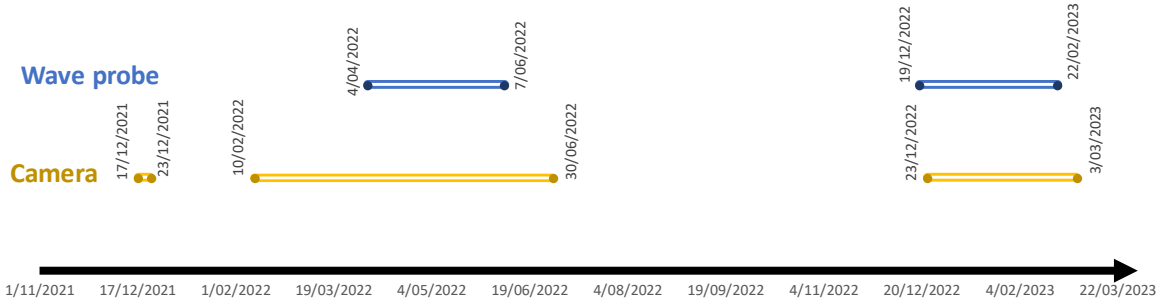

Figure 2.4 Data collection periods on the Clyde River

WRL also undertook an unmanned aerial vehicle (UAV) survey, which included the Manning River monitoring station on 23 March 2022 (Figure 2.5), in parallel with the initial camera and wave probe deployment. This survey data has been provided to DCCEEW in an accompanying .zip file.

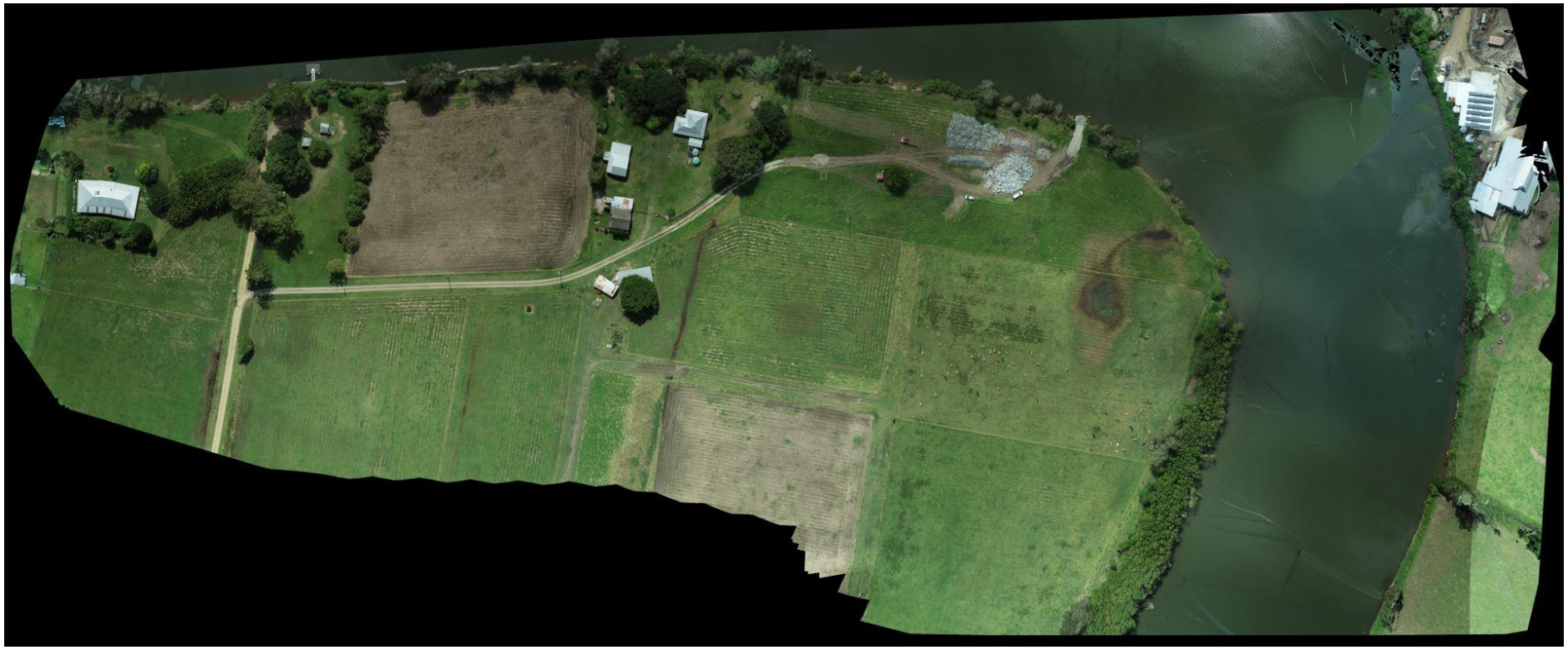

Figure 2.5 Orthomosaic image from UAV survey including Manning River monitoring station

3 Instrumentation and data processing

3.1 Cameras

Swift Enduro 4G trail cameras with 50 degree field of view (powered by a solar panel) were installed at both locations. Photographs of one of the trail cameras being tested at WRL prior to field deployment are shown in Figure 3.1. Photographs of the installed cameras on the Manning River and Clyde River are shown in Figure 3.2 and Figure 3.3, respectively.

The cameras were setup to automatically capture images at 30 minute increments between (and including) 7:00 am and 7:00 pm AEST and also to capture images upon motion trigger for boat detection. Images captured were then manually assessed for the presence of boats and/or boat waves, and positive detections were documented by WRL.

Figure 3.1 Photographs of an Enduro Swift 4G Trail Camera with solar panel prior to field deployment

Figure 3.2 Photograph of camera and solar panel installed on the Manning River

Figure 3.3 Photograph of camera and solar panel installed on the Clyde River

3.2 Wave probes

Battery powered RBRduo^3 wave probes (Figure 3.4), which logged data internally at 16 Hz at all times (i.e. 24 hours a day), were used to measure waves (which included wind waves and boat waves) at both locations. These wave probes were placed underwater inside a porous length of PVC pipe anchored on the riverbed approximately 5 to 10 m from the bank. Due to the proximity of wave probe to each bank, wave reflections off the bank were evident in the resulting dataset. The pressure transducers in the wave probes were located approximately 0.15 m above the riverbed at both locations. Photographs of the portable wave probe mounting rigs on the Manning River and Clyde River immediately prior to installation are shown in Figure 3.5 and Figure 3.6, respectively.

Figure 3.4 Photograph of RBRduo^3 wave probes prior to field deployment

Figure 3.5 Photograph of portable wave probe mounting rig used in the Manning River

Figure 3.6 Photograph of portable wave probe mounting rig used in the Clyde River

Following the conclusion of each wave probe deployment, the pressure sensor data was downloaded. Atmospheric pressure was subtracted from the raw pressure data which was then converted to water surface elevation time series using the technique of Nielsen (1989), reproduced in Equation 3.1.

$$\hat{\eta}_n = \frac{p_n}{\rho g} exp\left[A\left(\frac{y_p}{D}\right)\left(\frac{-p_{n-M} + 2p_n - p_{n+M}}{p_n g(M\delta)^2}\right)\left(D + \frac{p_n}{\rho g} - y_p\right)\right] \quad (3.1)$$

where

$\hat{\eta}_n$ = water surface elevation corresponding to the *n*th central gauge pressure reading (m)
p_n = the *n*th central gauge pressure reading (Pa)
ρ = water density (1024 kg/m^3)
g = acceleration due to gravity (9.81 m/s^2)
$M \approx \frac{\sqrt{\frac{D}{g}}}{\delta}$ (adopted integer values varied between 3 and 7)
δ = sampling period of data (0.06 s [16 Hz])
$A\left(\frac{y_p}{D}\right) = 0.67 + 0.34\frac{y_p}{D}$ (-)
y_p = height of the pressure transducer above the river bed (0.15 m)
D = water depth (m)

At both the Manning River and the Clyde River, the wave probes were deployed in water depths up to approximately 2.15 m. In addition to wave action, water levels varied under the influence of tides and freshwater flows. At both locations, the wave probes became emergent on very low tides. Wave data was not analysed for periods when the wave probe was less than 0.3 m below the water surface due to sensor limitations.

A high-pass filter of 0.1 Hz (i.e. wave periods longer than 10 s) was applied to remove the tidal signal. A low-pass filter of 1.5 Hz (i.e. wave periods shorter than 0.7 s) was also applied to remove very short wave periods which are outside the range of validity for the Nielsen (1989) technique.

Zero-crossing analysis was used to determine the height and period of each individual wave measured by the wave probe. The energy of each individual wave was calculated using Equation 3.2 (Maynord, 2001).

$$E = \frac{\rho g^2 H^2 T^2}{16\pi} \quad (3.2)$$

where

E = wave energy (per unit wave-crest length) (kg.m/s^2 or J/m)
ρ = water density (1024 kg/m^3)
g = acceleration due to gravity (9.81 m/s^2)
H = wave height (m)
T = wave period (s)
π = constant (≈ 3.14)

4 Results

4.1 Measured wave climate

Four summary plots of the measured wave climate from all the wave probe deployments at both sites were produced as follows:

- Wave height versus wave period (Manning - Figure 4.1; Clyde - Figure 4.5)
- Wave energy versus wave period (Manning - Figure 4.2; Clyde - Figure 4.6)
- Wave height versus exceedance probability (Manning - Figure 4.3; Clyde - Figure 4.7)
- Wave energy versus exceedance probability (Manning - Figure 4.4; Clyde - Figure 4.8)

While it was was outside the scope of works of this study to attribute the generation source for each of the measured waves, the following sources are considered likely for the two monitoring sites:

- 0.7 s to 1.5 s wave period: wind waves and boat waves
- 1.5 s to 7 s wave period: boat waves
- 7 s to 10 s wave period: generation source unknown

To illustrate the wave conditions which may be generated by strong winds blowing along the longest fetches to the Manning River (approximate fetch: 1,300 m from the south) and Clyde River (approximate fetch: 400 m from the north-northeast) sites, the significant wave height and peak wave period calculated for two example wind speeds is shown in Table 4.1.

Table 4.1 Example wind wave conditions calculated for two different wind gust speeds

Monitoring site	Fetch (m)	3 s gust wind speed (km/hour)	Significant wave height (m)	Peak wave period (s)
Manning River	1,300 (S)	50	0.17	1.3
		80	0.29	1.5
Clyde River	400 (NNE)	50	0.10	0.9
		80	0.18	1.1

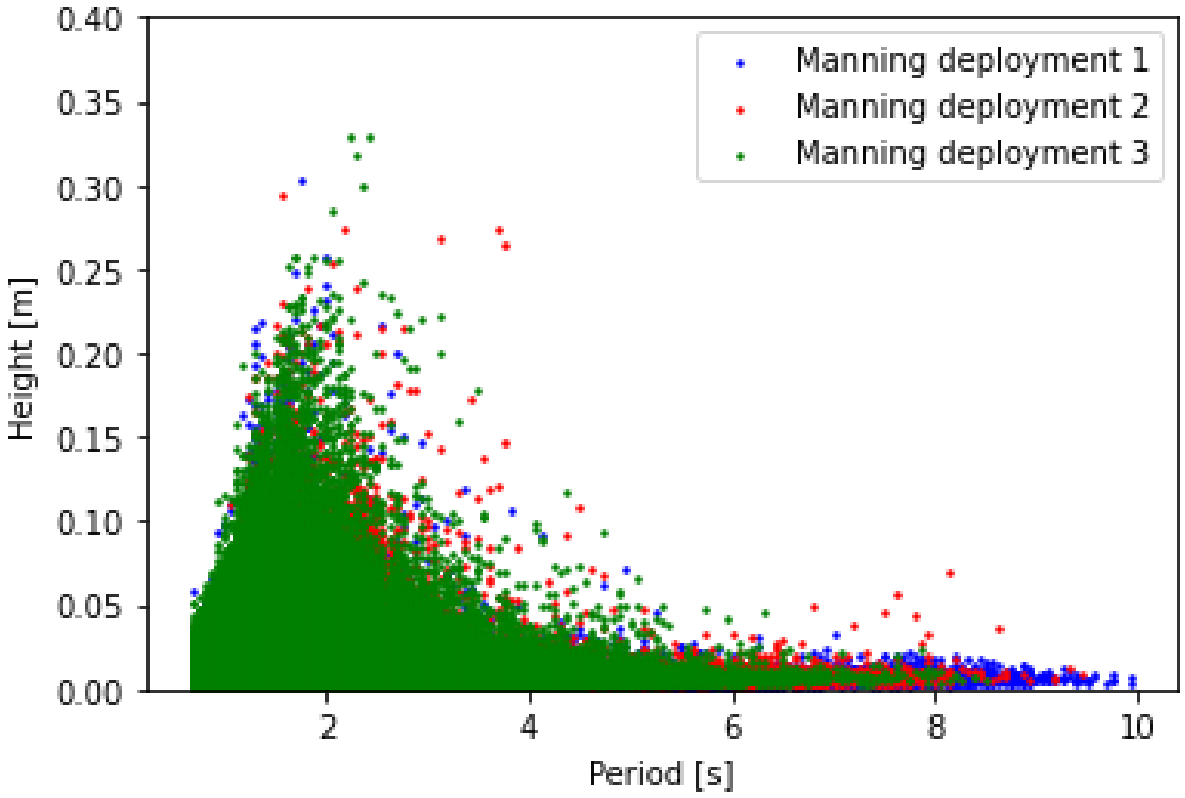

Figure 4.1 Scatter plot of wave height versus period at the Manning River monitoring station

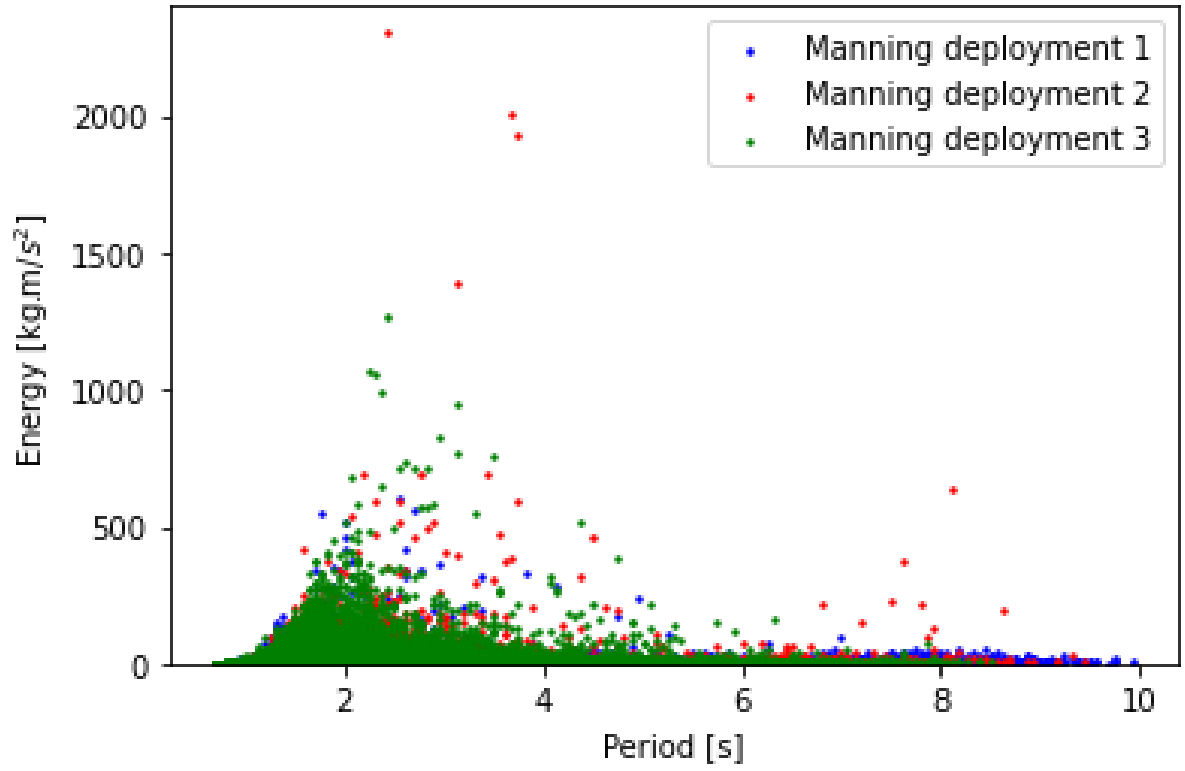

Figure 4.2 Scatter plot of wave energy versus period at the Manning River monitoring station

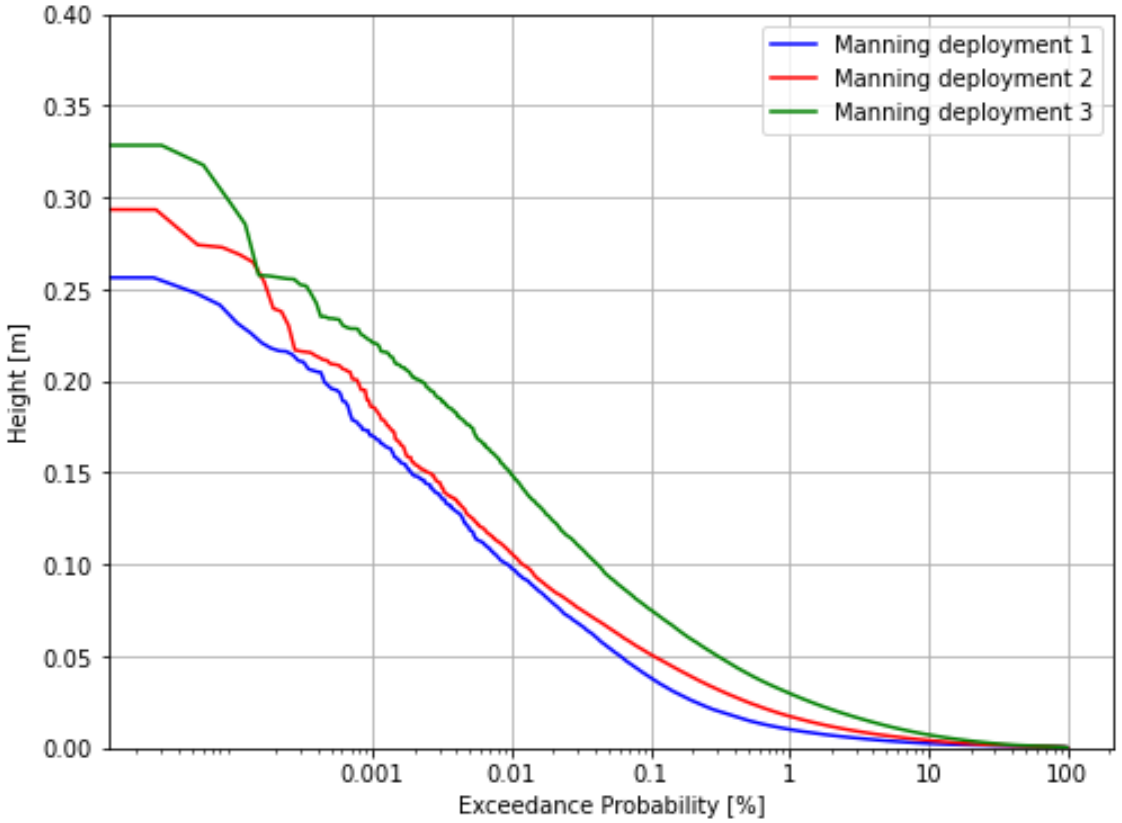

Figure 4.3 Exceedance probability of wave height at the Manning River monitoring station

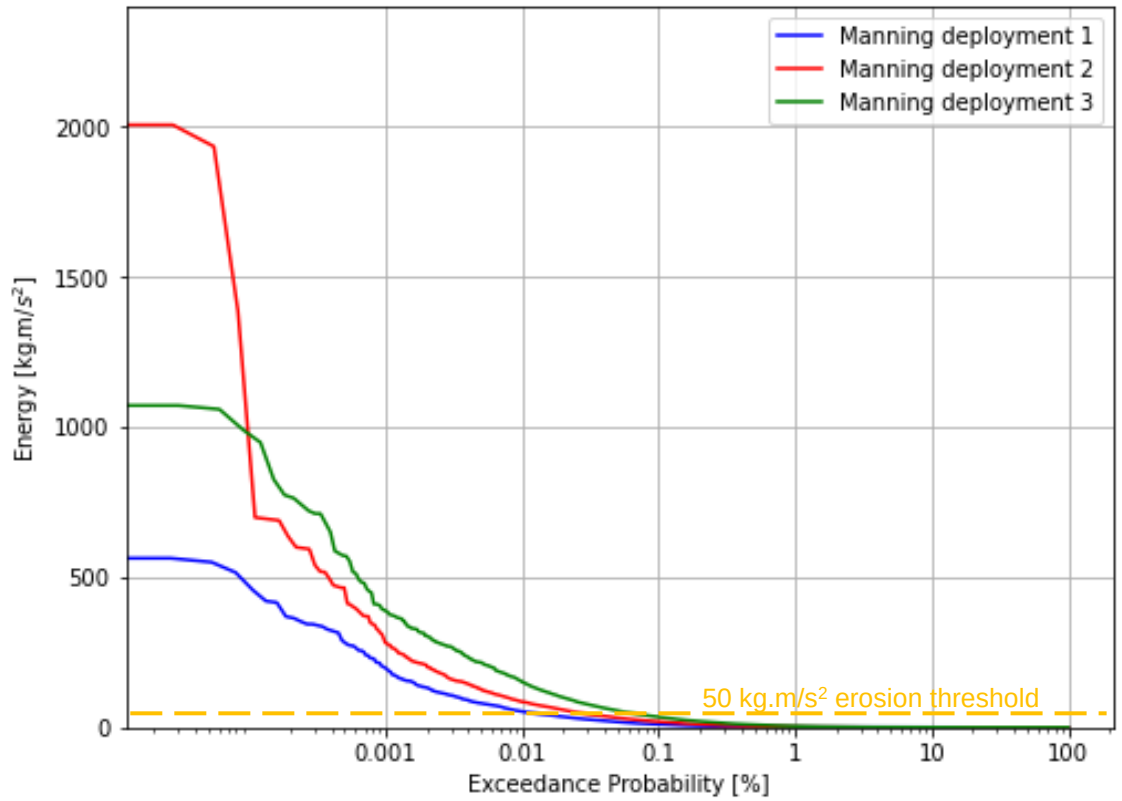

Figure 4.4 Exceedance probability of wave energy at the Manning River monitoring station

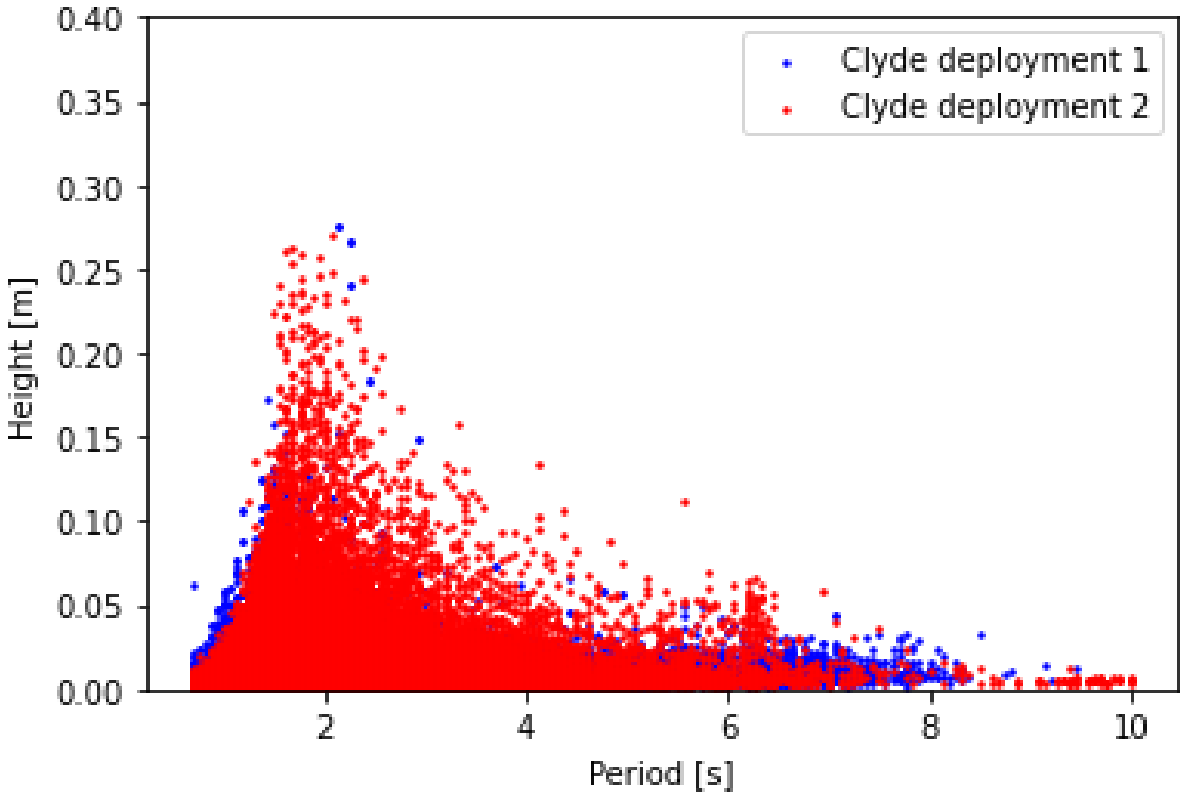

Figure 4.5 Scatter plot of wave height versus period at the Clyde River monitoring station

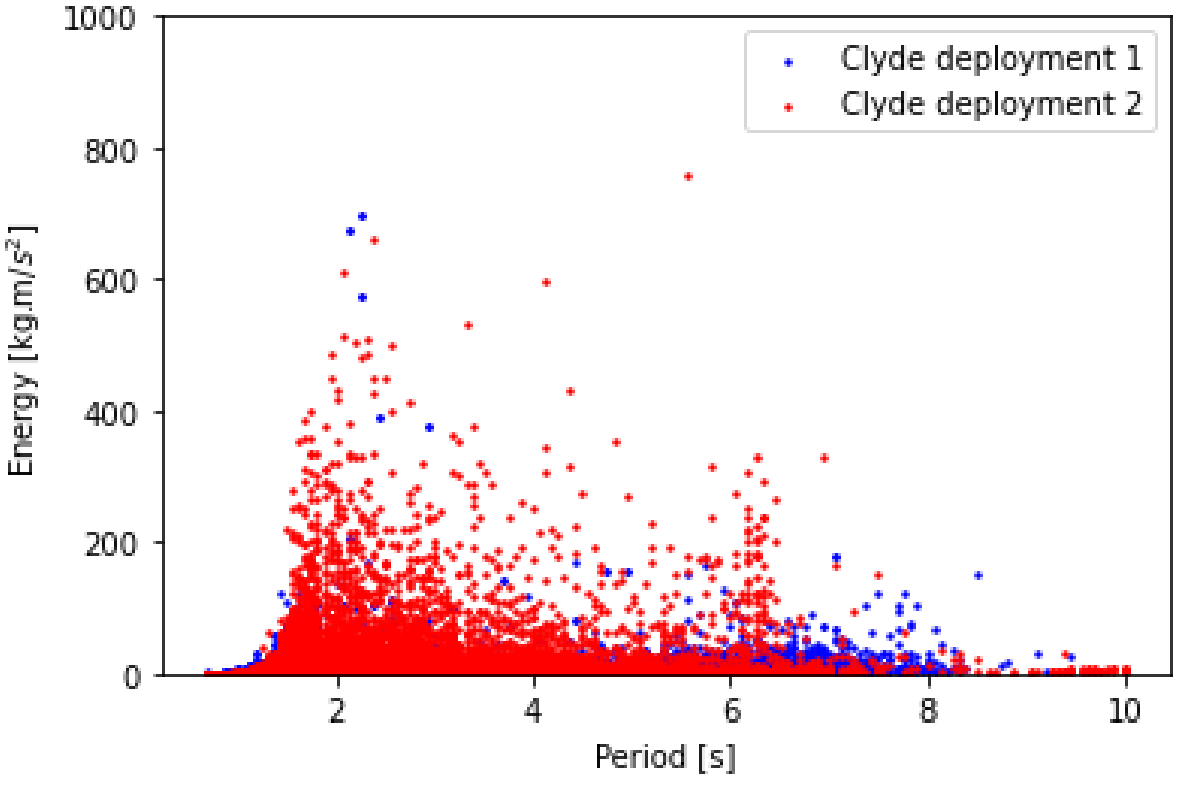

Figure 4.6 Scatter plot of wave energy versus period at the Clyde River monitoring station

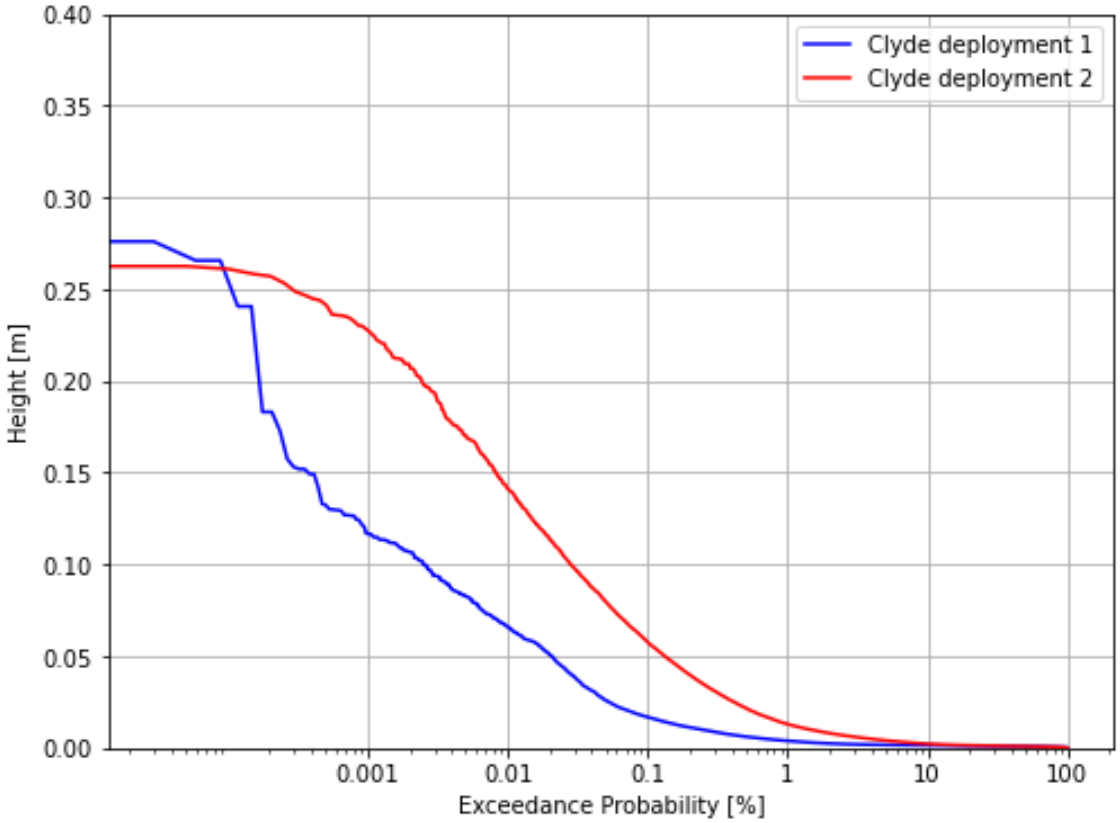

Figure 4.7 Exceedance probability of wave height at the Clyde River monitoring station

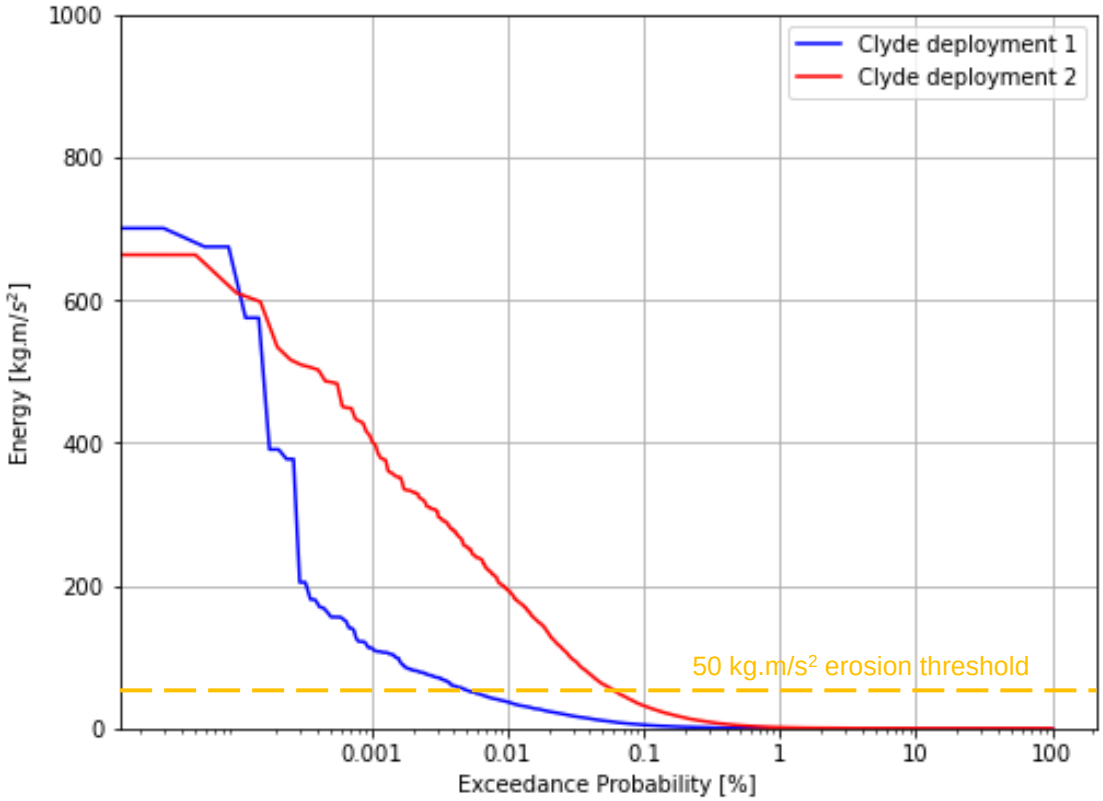

Figure 4.8 Exceedance probability of wave energy at the Clyde River monitoring station

The observed ambient wave climate was very calm at the Manning River monitoring station. Only 1% of wave heights exceeded 0.03 m for the three Manning River deployments, with a maximum wave height of 0.33 m (Manning deployment 3). While this percentage is based on the number of waves and not the percentage of time, it is a reasonable approximation that for the vast majority of time, wave heights are less than a ripple. The highest waves (greater than 0.25 m) had periods ranging between approximately 1.5 and 4.0 s. While waves with longer periods (above 5 s) were evident in the data, their associated wave heights were smaller (less than 0.10 m). Manning deployment 3 (covering the 2022-23 summer) had the greatest proportion of higher wave heights. The maximum individual wave energy for each of the Manning River deployments varied between approximately 600 kg.m/s^2 (Manning deployment 1; see also Figure 4.13) and 2,000 kg.m/s^2 (Manning deployment 2).

The observed ambient wave climate was similarly very calm at the Clyde River monitoring station. Only 1% of wave heights exceeded 0.02 m for the two Clyde River deployments, with a maximum wave height of 0.28 m (Clyde deployment 1; see also Figure 4.19). The highest waves (greater than 0.25 m) had a narrower range of periods between approximately 1.5 and 2.5 s. Longer period waves with small wave heights were also evident in the Clyde records. Clyde deployment 2 (covering the 2022-23 summer) generally had the greatest proportion of higher wave heights. The maximum individual wave energy for both Clyde River deployments were similar at approximately 700 kg.m/s^2 (see Figure 4.19).

4.2 Boats detected by camera

Over the camera monitoring period on the Manning River (23 March 2022 to 14 December 2022), a total of 244 images captured a boat and/or a boat wave as summarised by calendar month in Table 4.2. A selection of 16 boat images on the Manning River are shown in Figure 4.9 and Figure 4.10.

Note that this camera became tilted on 1 April 2022 due to flood impacts and was not straightened again until 27 April 2022 (with an additional adjustment on 9 May 2022).

Note also that boat detections are very likely to be under-represented for September to December due to an error in camera timing resulting in recording only between 7:00 pm and 10:00 pm AEST (i.e. approximately 2 hours of daylight) from 15 September 2022 to 13 October 2022 and from 4 November 2022 until its retrieval on 14 December 2022.

Table 4.2 Summary of boat and boat wave images captured on the Manning River

Calendar month	# images with boat	# images with boat wave only	# images with boat and/or boat wave
23-31/03/2022	0	0	0
1-30/04/2022	34	9	43
1-31/05/2022	30	1	31
1-30/06/2022	80	0	80
1-31/07/2022	19	0	19
1-31/08/2022	36	3	39
1-30/09/2022	21	0	21
1-31/10/2022	5	0	5
1-30/11/2022	6	0	6
1-14/12/2022	0	0	0
TOTAL	**231**	**13**	**244**

Over the three camera monitoring periods on the Clyde River (17 December 2021 to 23 December 2021, 10 February 2022 to 30 June 2022 and 23 December 2022 to 3 March 2023), a total of 20 images captured a boat and/or a boat wave as summarised by calendar month in Table 4.3. A selection of eight boat images on the Clyde River is shown in Figure 4.11.

Table 4.3 Summary of boat and boat wave images captured on the Clyde River

Calendar month	# images with boat	# images with boat wave only	# images with boat and/or boat wave
17-23/12/2021	2	0	2
10-28/02/2022	2	5	7
1-31/03/2022	3	0	3
1-30/04/2022	1	1	2
1-31/05/2022	1	1	2
1-30/06/2022	1	1	2
23-31/12/2022	1	0	1
1-31/01/2023	1	0	1
1-28/02/2023	0	0	0
1-3/03/2023	0	0	0
TOTAL	**12**	**8**	**20**

While the width of the river is similar at both sites (approximately 100 m), a greater proportion of positive detections on the Clyde River contained a boat wave only (i.e. the boat was out of the frame). This is considered to be due to the camera orientation; the Clyde River camera was oriented more perpendicular to the bank while the Manning River camera was oriented more downstream (allowing a passing boat to stay in the frame for longer after motion detection).

The majority of positive boat and boat wave detections at both sites were triggered by motion detection (rather than the automatic images every 30 minutes). However, many images were triggered by motion other than from a passing boat, such as floating birds (i.e. false positives). While some waves which appeared likely to have been generated by a boat in the measured time series (occurring between 7:00 am and 7:00 pm AEST) did not have an accompanying image, an assessment of the number of passing boats missed by the camera (i.e. false negatives) was outside the scope of works of this study.

Figure 4.9 Selection of boat images captured on the Manning River (1 of 2)

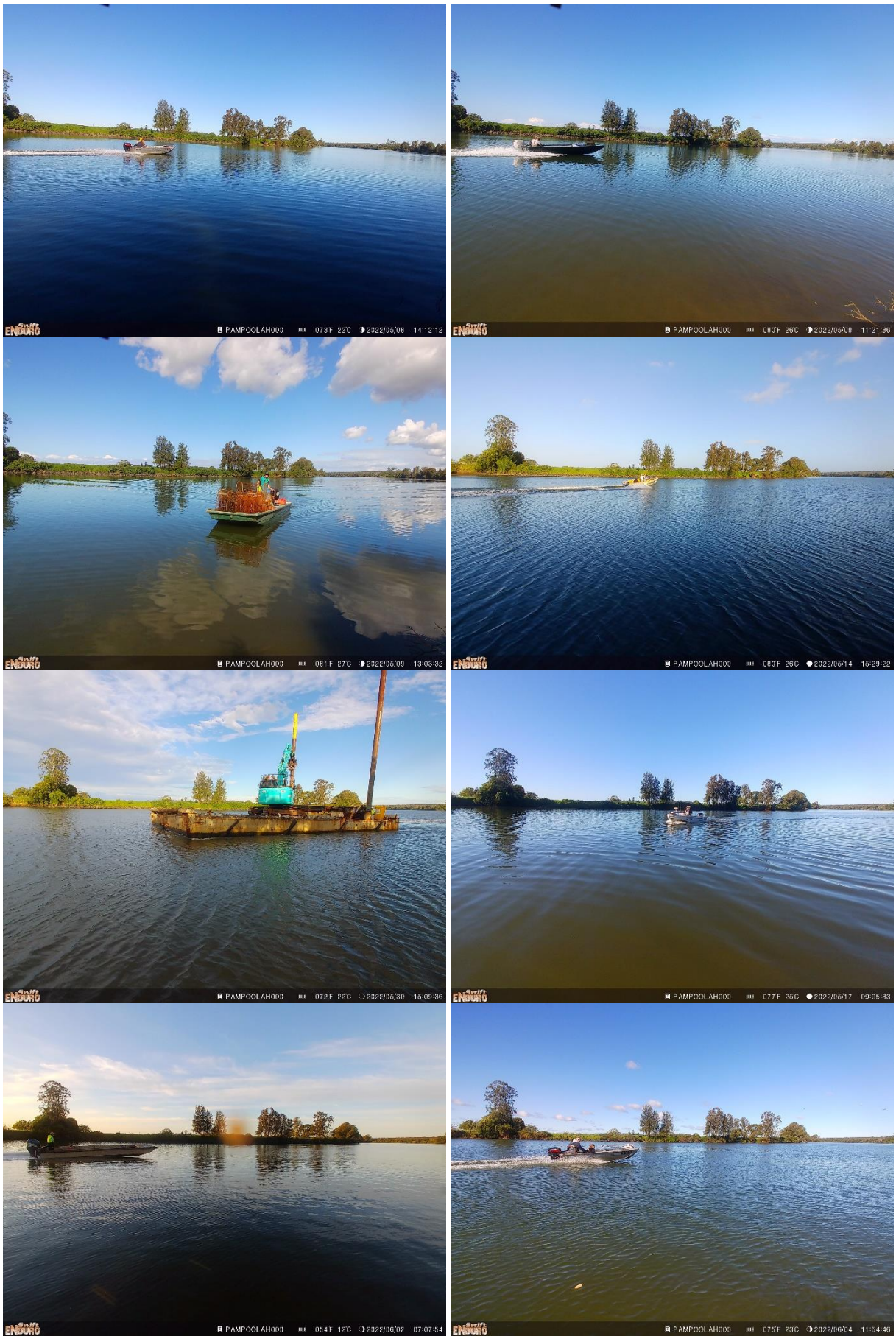

Figure 4.10 Selection of boat images captured on the Manning River (2 of 2)

Figure 4.11 Selection of boat images captured on the Clyde River

4.3 Example wave traces for individual boats

While it was was outside the scope of works of this study to analyse waves associated with every individual boat pass, further analysis was undertaken on a selection of seven boats passing the Manning River monitoring station and one boat passing the Clyde River monitoring station. Figures 4.12 to 4.19 show example photos captured of each boat and their associated measured wave trace along with the following wave parameters:

- Number of waves within each wave packet generated by passing vessel (Count)
- Maximum wave height (H_{max})
- Period of maximum wave height (T_{Hmax})
- Energy of maximum wave height (E_{Hmax})
- Maximum wave period (T_{max})
- Maximum individual wave energy (E_{max})
- Total wave energy of the wave train (E_{total}).

On each wave trace plot, the wave with maximum height (H_{max}) is shaded blue, the wave with maximum period (T_{max}) is shaded orange and the wave with maximum energy (E_{max}) is shaded green. If a wave within the trace is identified with more than one of these parameters, the shadings are stacked.

Note that E_{total} was determined by simply summing the calculated energy for each individual wave within the wave train.

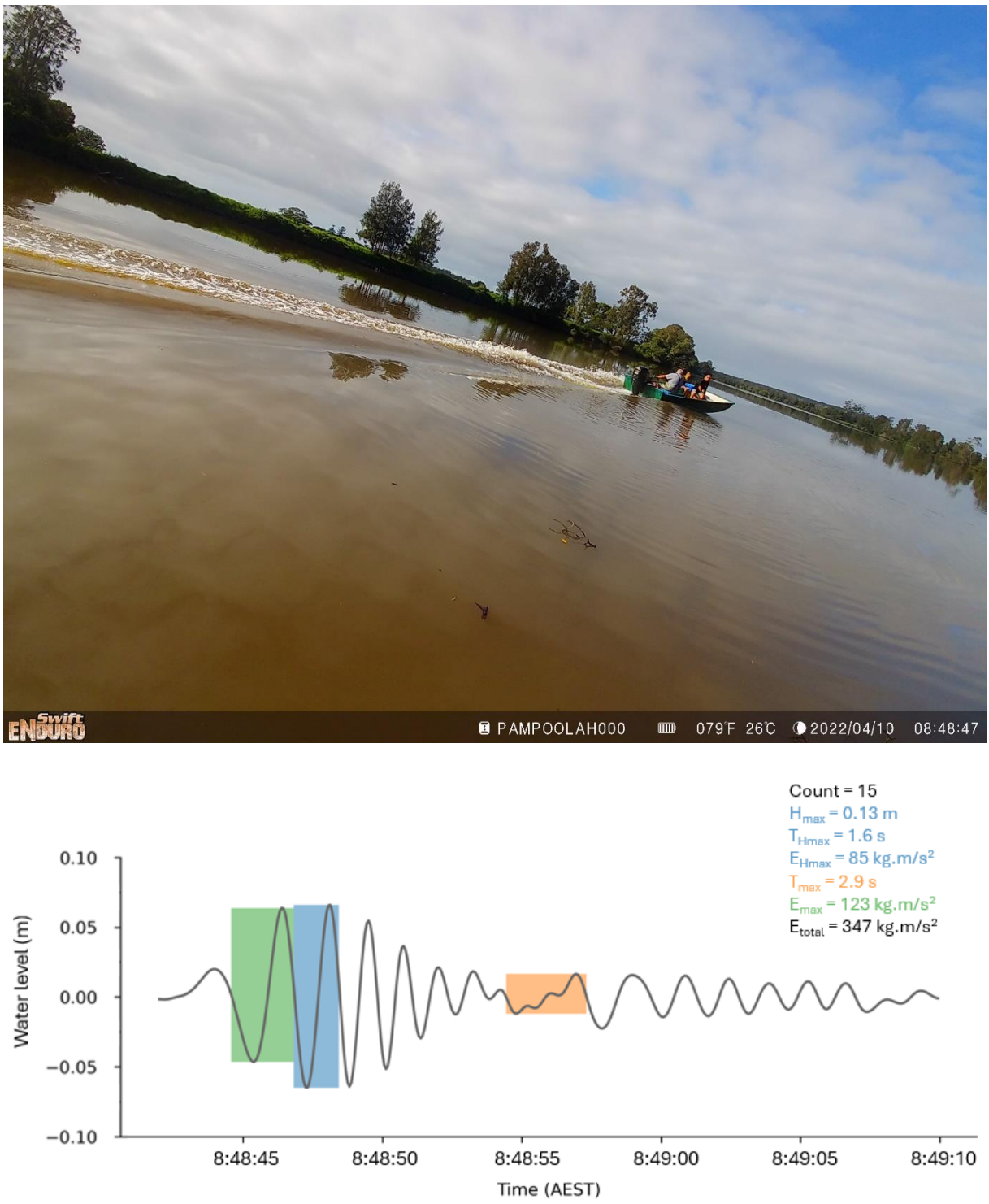

Figure 4.12 Example wave trace from boat heading downstream on Manning River (image 10 April 2022 8:48:47 AEST - wave probe deployment 1)

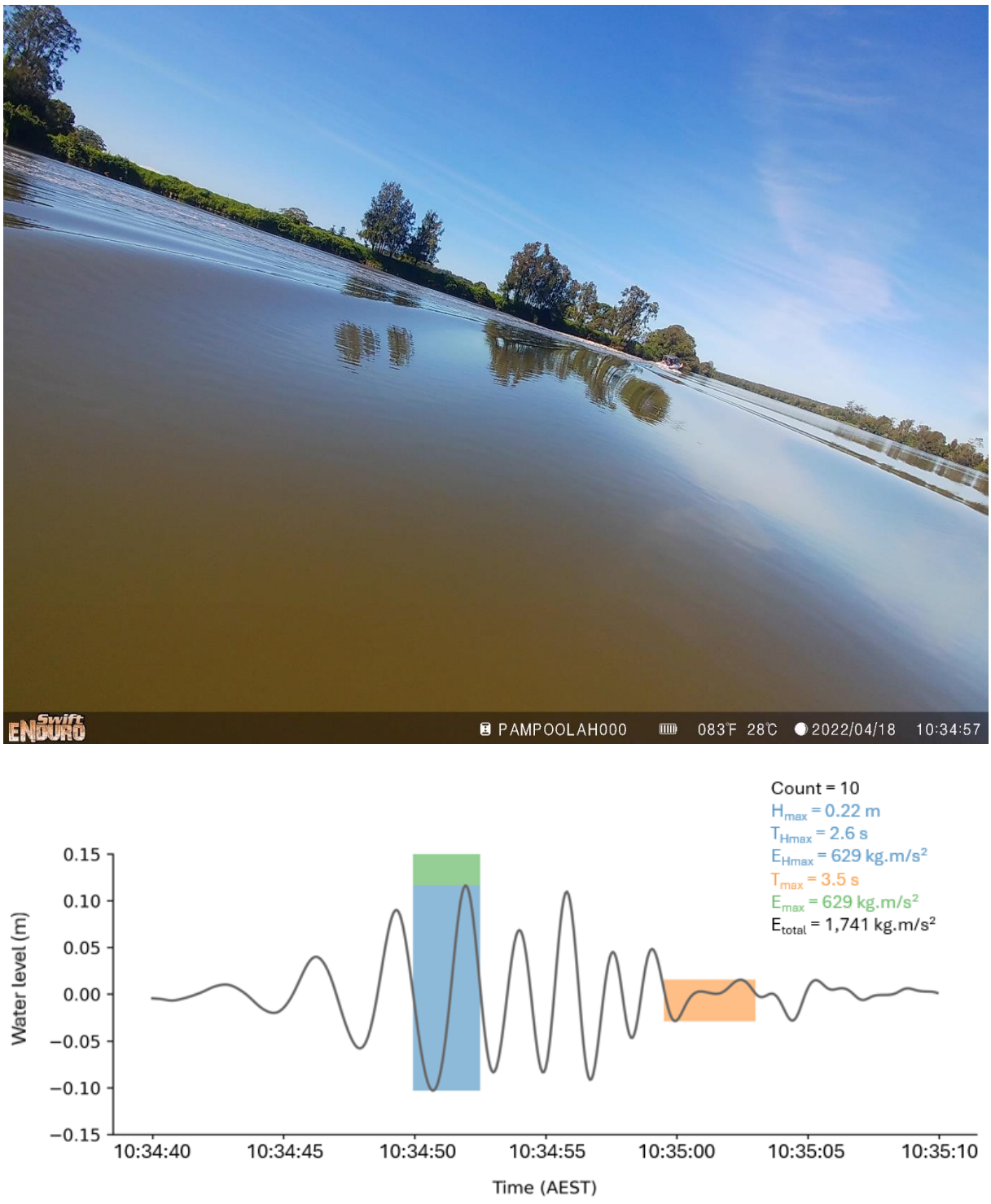

Figure 4.13 Example wave trace from boat heading downstream on Manning River (image 18 April 2022 10:34:57 AEST - wave probe deployment 1)

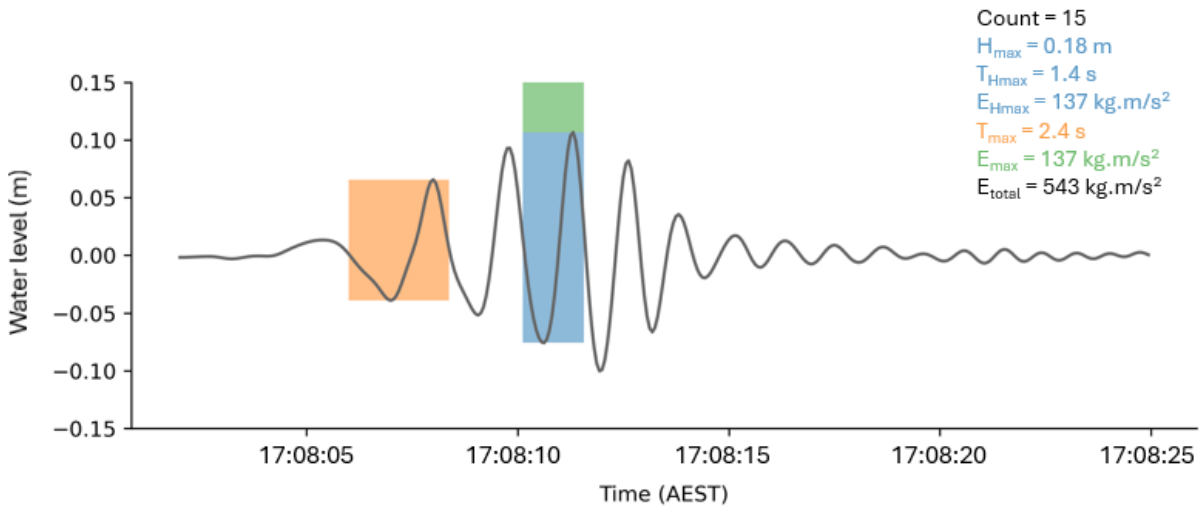

Figure 4.14 Example wave trace from boat heading downstream on Manning River (image 29 April 2022 17:08:09 AEST - wave probe deployment 1)

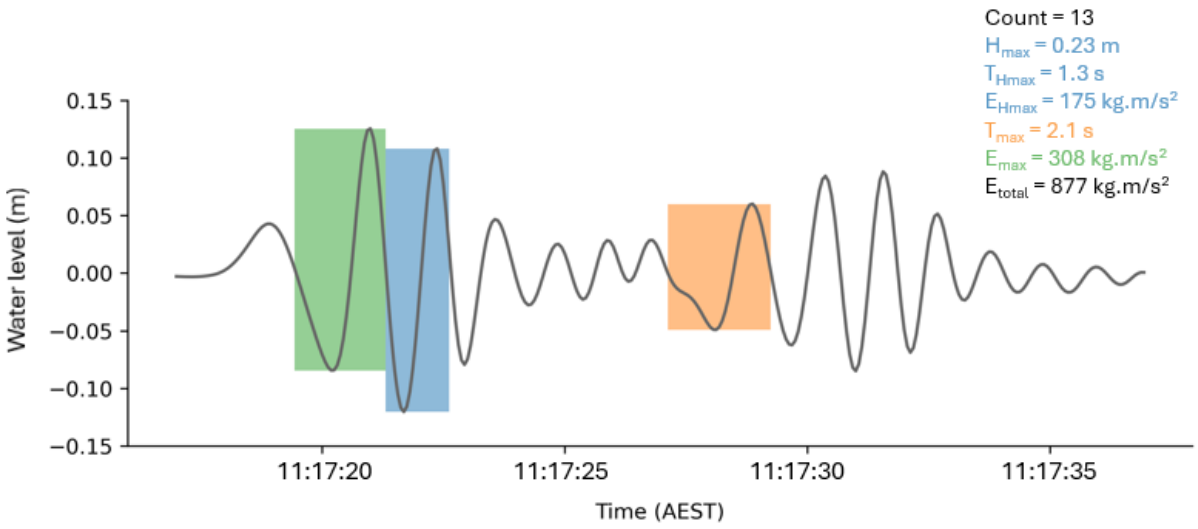

Figure 4.15 Example wave trace from boat heading downstream on Manning River (image 11 May 2022 11:17:23 AEST - wave probe deployment 1)

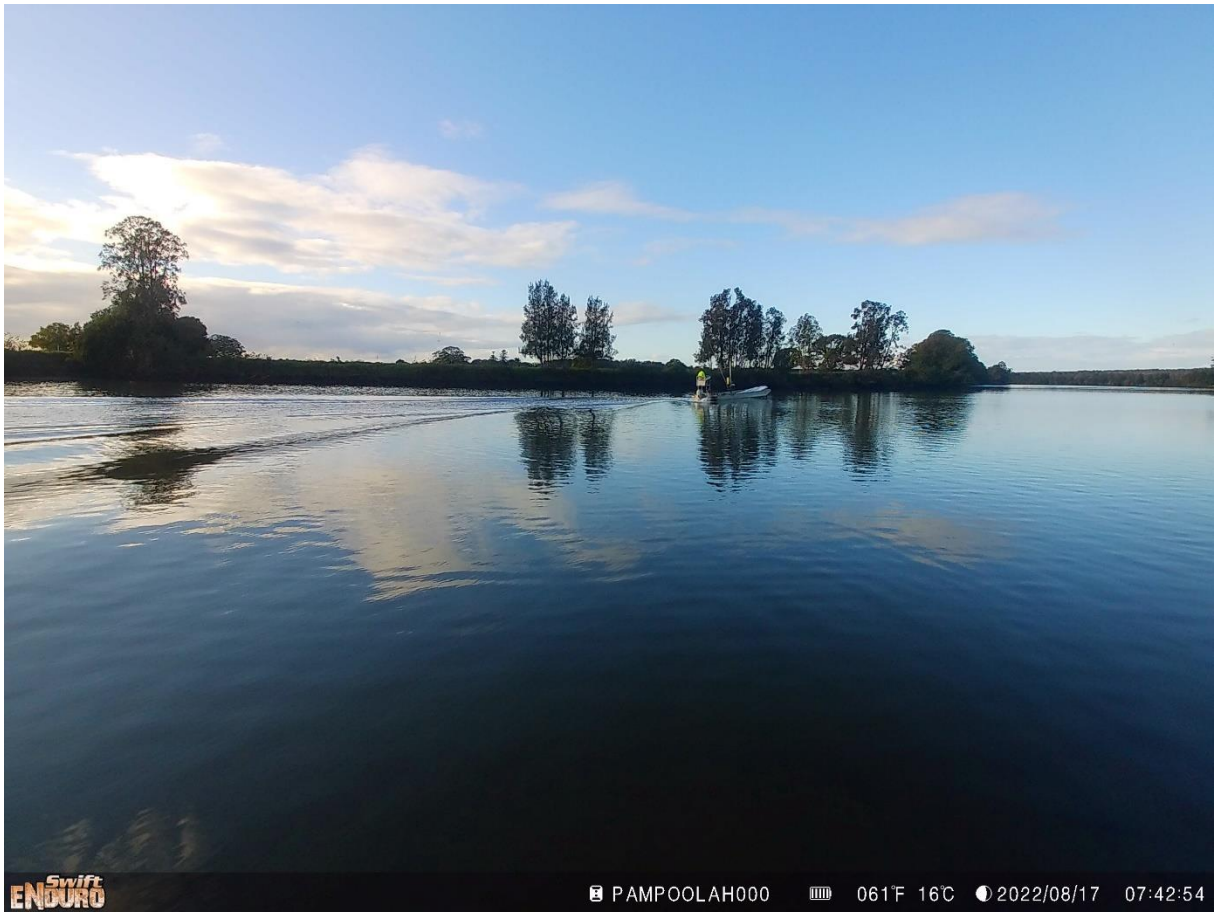

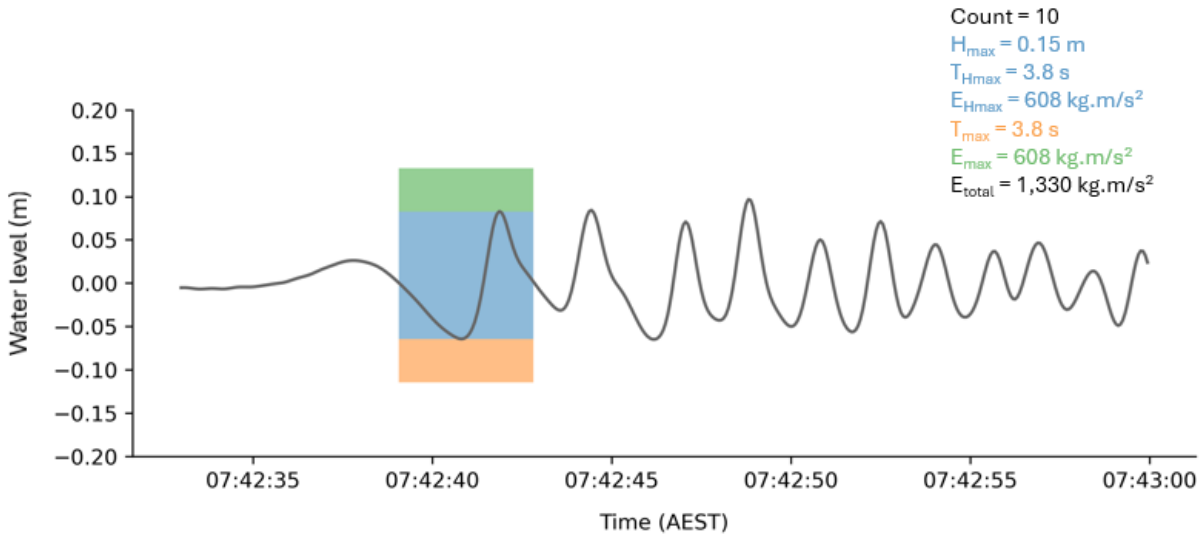

Figure 4.16 Example wave trace from boat heading downstream on Manning River (image 17 Aug 2022 7:42:54 AEST - wave probe deployment 2)

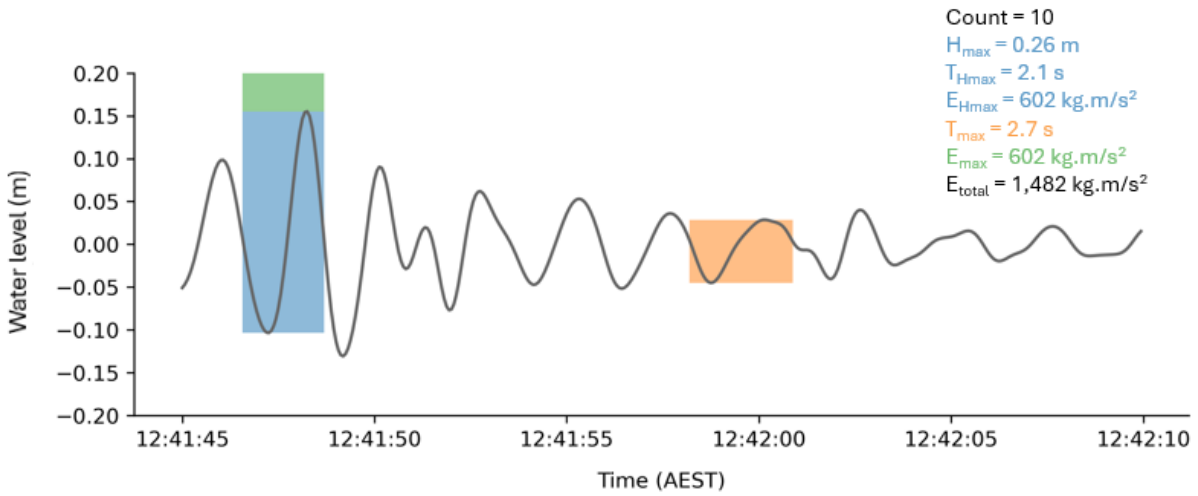

Figure 4.17 Example wave trace from boat heading upstream on Manning River (image 18 Aug 2022 12:41:54 AEST - wave probe deployment 2)

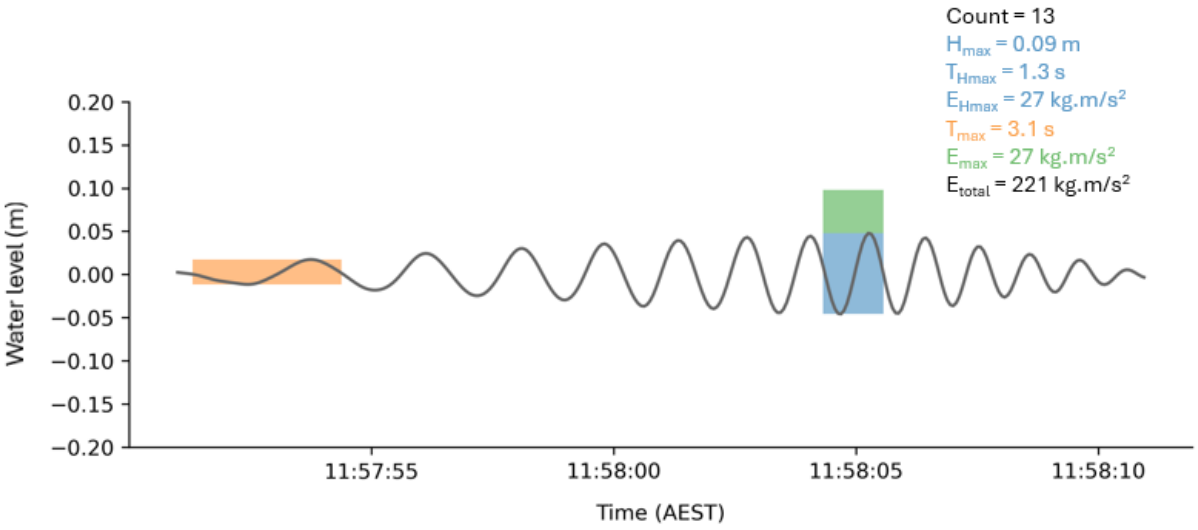

Figure 4.18 Example wave trace from boat heading downstream on Manning River (image 21 Aug 2022 11:58:01 AEST - wave probe deployment 2)

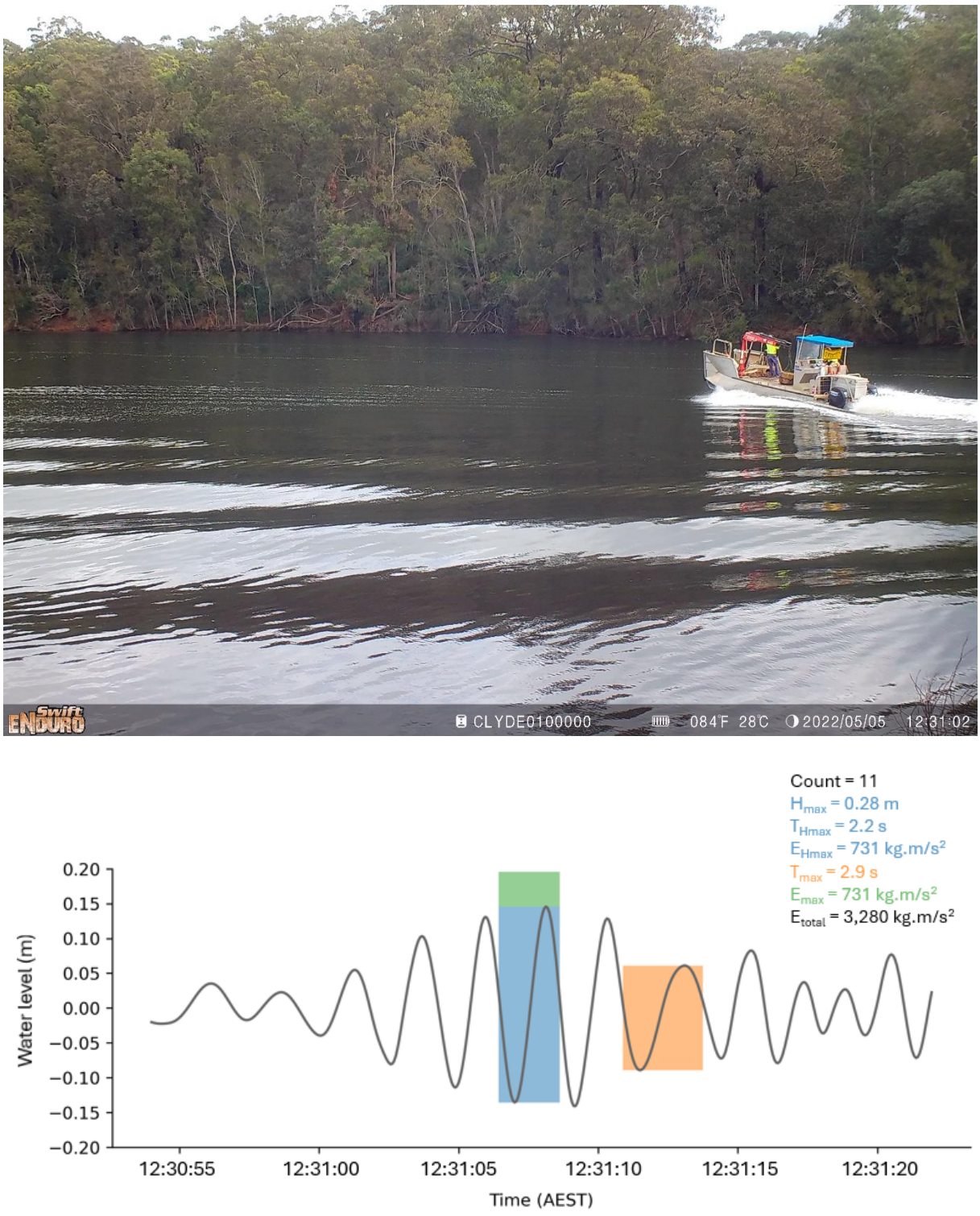

Figure 4.19 Example wave trace from boat heading downstream on Clyde River (image 5 May 2022 12:31:02 AEST - wave probe deployment 1)

5 Discussion

WRL understands that DCCEEW and LLS have monitored bank erosion, in parallel with this local wave climate investigation, at the same two locations on the Manning River and Clyde River. To assess the potential for bank erosion from the local wave climate, wave height should not be considered in isolation of wave period. Small waves with long periods have the potential to cause erosion. It is preferable to assess the potential for bank erosion using wave energy (which considers both wave height and wave period). A general erosion threshold value for wave energy does not exist, however, the following site-specific thresholds have been adopted in other Australian locations (considering the local sediments, turbidity, bathymetry, tidal range, wind climate, boating activity, etc.):

- Gordon River, Tasmania (Cox and Macfarlane, 2019): 30 kg.m/s^2 (no erosion)
- Noosa River, Queensland (Macfarlane and Cox, 2002): 60 kg.m/s^2 (low erosion)
- Brisbane River, Queensland (Macfarlane and Cox, 2002): 180 kg.m/s^2 (low erosion)

The Gordon River is a highly controlled environment (recreational boating is prohibited and commercial tourist operations are licenced and monitored) and the value of 30 kg.m/s^2 was set to prevent any erosion from boat activity. Cognisant of existing boating activity, the values for the Noosa River and Brisbane River are higher and were set to result in low erosion, rather than no erosion.

In the absence of further detailed studies at the Manning River and Clyde River sites, WRL considers that bank erosion potential exists for individual waves with energy greater than approximately 50 kg.m/s^2. As an example, this energy equates to individual waves with the following parameters:

- 0.16 m height with 1.0 s period
- 0.08 m height with 2.0 s period
- 0.04 m height with 4.0 s period.

It is acknowledged that while wave energy is constant for each of these example waves, the form (e.g. spilling, plunging, collapsing, surging) in which they break on a bank will vary.

As shown in Figure 4.4 and Figure 4.8, less than 0.1% of waves measured during the deployments at the Manning River and Clyde River sites had wave energy with the potential to cause bank erosion (greater than 50 kg.m/s^2). However, although only a very small proportion of waves exceeded this erosion potential threshold, the largest waves recorded at the Manning River (2,000 kg.m/s^2) and Clyde River (700 kg.m/s^2) sites were an order of magnitude higher than this value.

6 Summary

WRL was engaged by DCCEEW to partner in developing and implementing a pilot field program to measure the local wave climate and automatically photograph boat traffic at one location on the Manning River and another location on the Clyde River for LLS. This report has summarised the data collected at these two monitoring stations between December 2021 and March 2023.

The observed ambient wave climate was very calm at both monitoring stations for almost the entire recording period (99% of waves were less than 0.03 m high on the Manning and less than 0.02 m on the Clyde). The highest waves (greater than 0.25 m) had periods between 1.5 and 4.0 s on the Manning River and between 1.5 and 2.5 s on the Clyde River. Based on the expected range of wave periods for wind waves at these sites and the typical range of boat wave periods, the highest and most energetic waves at both monitoring sites are generated by passing boats.

The highest individual waves and maximum individual wave energy were recorded on the Manning River, although maxima values on the Clyde River were not significantly lower. Although only a very small proportion of waves (less than 0.1%) measured during the deployments at the Manning River and Clyde River sites had wave energy with the potential to cause bank erosion (greater than 50 kg.m/s^2), the largest waves recorded at the Manning River (2,000 kg.m/s^2) and Clyde River (700 kg.m/s^2) sites were an order of magnitude higher than this indicative erosion threshold value. The deployments covering the 2022-23 summer period at both sites had the greatest proportion of higher wave heights.

There were significantly more boats (and/or boat waves) detected on the Manning River (244) compared to the Clyde River (20) during the data collection program. Detailed wave analysis for eight individual passing boat events (confirmed by photo capture) was conducted and key wave parameters regarding the height, period and energy of the waves were documented. In four of these examples, the maximum individual wave energy generated by each boat was greater than 600 kg.m/s^2.

7 References

Cox, G & Macfarlane, GJ 2019, 'The effects of boat waves on sheltered waterways-thirty years of continuous study', In Australasian Coasts and Ports 2019 Conference: Future directions from 40°S and beyond, Hobart, 10-13 September 2019.

Macfarlane, GJ & Cox, G 2002, Vessel Wash Impacts on Bank Erosion – Noosa River Between Lake Cootharaba and Lake Cooroibah – Brisbane River Kookaburra Park to the Bremer River Junction, Report Number 01/G/18, AMC Search Limited, Launceston.

Maynord, ST 2001, 'Boat Waves on Johnson Lake and Kenai River, Alaska', Coastal and Hydraulic Laboratory Report Number ERDC/CHL TR-01-31, US Army Corps of Engineers.

Nielsen , P 1989, 'Analysis of Natural Waves by Local Approximations', ASCE Journal of Waterway, Port, Coastal and Ocean Engineering, Volume 115, Number 3, May, pp. 384-397.